

Data on face-to-face contacts in an office building suggest a low-cost vaccination strategy based on community linkers

MATHIEU GÉNOIS, CHRISTIAN L. VESTERGAARD and JULIE FOURNET

Aix Marseille Université, Université de Toulon, CNRS, CPT, UMR 7332, 13288 Marseille, France
(e-mail: genois@cpt.univ-mrs.fr)

ANDRÉ PANISSON

Data Science Laboratory, ISI Foundation, Torino, Italy

ISABELLE BONMARIN

Département des maladies infectieuses, Institut de veille sanitaire, Saint-Maurice, France

ALAIN BARRAT

Aix Marseille Université, Université de Toulon, CNRS, CPT, UMR 7332, 13288 Marseille, France
and
Data Science Laboratory, ISI Foundation, Torino, Italy

Abstract

Empirical data on contacts between individuals in social contexts play an important role in providing information for models describing human behavior and how epidemics spread in populations. Here, we analyze data on face-to-face contacts collected in an office building. The statistical properties of contacts are similar to other social situations, but important differences are observed in the contact network structure. In particular, the contact network is strongly shaped by the organization of the offices in departments, which has consequences in the design of accurate agent-based models of epidemic spread. We consider the contact network as a potential substrate for infectious disease spread and show that its sparsity tends to prevent outbreaks of rapidly spreading epidemics. Moreover, we define three typical behaviors according to the fraction f of links each individual shares outside its own department: residents, wanderers, and linkers. Linkers ($f \sim 50\%$) act as bridges in the network and have large betweenness centralities. Thus, a vaccination strategy targeting linkers efficiently prevents large outbreaks. As such a behavior may be spotted *a priori* in the offices' organization or from surveys, without the full knowledge of the time-resolved contact network, this result may help the design of efficient, low-cost vaccination or social-distancing strategies.

Keywords: *complex networks, temporal networks, sociophysics, epidemiology*

1 Introduction

Data-driven models of disease propagation are essential tools for the prediction and prevention of epidemic outbreaks. Thanks to important increases in data availability and computer power, highly detailed agent-based models have in particular become widely used to describe epidemic spread at very different scales, from small communities to a whole country or continent (Davey et al., 2008; Ajelli

et al., 2010; Ajelli et al., 2014; Merler & Ajelli, 2010). One of the interests of such approaches comes from the level of detail they entail in the description of a disease propagation, from the amount of information they provide on the risk supported by each population category and on the probabilities of occurrence of transmission events in different circumstances. Moreover, the range of modeling possibilities is very large, and many different assumptions can be tested on how individuals come in contact, how a disease is transmitted and how such transmission can be contained. The drawback of this freedom in the model design lies in a certain arbitrariness in modeling choices. In order to alleviate this arbitrariness, models need to be fed with information and data concerning population statistics and individual behavior. In this respect, a crucial point regards the way in which people interact in their day-to-day life, and how these interactions affect disease propagation (Mossong et al., 2008; Read et al., 2012). The collection of detailed data sets of human interactions is highly needed, as well as the extraction of the most relevant stylized characteristics and statistical features of these interactions (Stehlé et al., 2011b; Blower & Go, 2011; Machens et al., 2013; Barrat et al., 2013; Barrat et al., 2014). Understanding which features of human contact patterns are most salient can also help design low-cost methods based on limited information for targeted intervention strategies (Lee et al., 2012; Smieszek & Salathé, 2013; Chowell & Viboud, 2013; Gemmetto et al., 2014).

In order to develop our knowledge and understanding of human interactions, novel techniques based on sensors using Wi-Fi, Bluetooth or RFID have emerged in the last decade and have provided important new insights (Zhang et al., 2012; Vu et al., 2010; Eagle et al., 2009; Stopczynski et al., 2014; Cattuto et al., 2010; Barrat et al., 2014; Salathé et al., 2010). In the present article, we consider data on face-to-face contacts collected using wearable sensors (Cattuto et al., 2010; Barrat et al., 2014). The corresponding infrastructure, developed by the SocioPatterns collaboration (www.sociopatterns.org), allows obtaining time-resolved data on close face-to-face proximity events between individuals, yielding information not only on the overall network formed by these contacts, but also on the dynamics of these interactions. Previous works have shown that many properties of these dynamics—contact times, inter-contact times, number of contacts per link, etc—have broad statistical distributions and display robust features across several contexts: schools (Salathé et al., 2010; Stehlé et al., 2011a; Fournet & Barrat, 2014), hospitals (Isella et al., 2011a; Vanhems et al., 2013), museums (Isella et al., 2011b) or conferences (Isella et al., 2011b; Barrat et al., 2013; Stehlé et al., 2011b). On the other hand, the contact networks also exhibit different high-level structures in each specific context, which can influence the way epidemics spread (Isella et al., 2011b; Machens et al., 2013; Gauvin et al., 2013; Gauvin et al., 2014). Here we consider the contact patterns between adults at work, which have been less studied in an epidemiological perspective, even if the influence of office spatial layouts on social interactions has been considered from a sociological and architectural perspective (Penn et al., 1999; Sailer & McCulloh, 2012; Brown et al., 2014b; Brown et al., 2014a). *A priori*, the workplace is one of the locations where adults spend most of their time and, as such, may represent an important spot for transmission of diseases between adults (Ajelli et al., 2010). We therefore present an analysis of the human contact network in such a place, namely a building of the *Institut de veille sanitaire* (InVS, French Institute for Public Health Surveillance). We first discuss how the organization of the offices

Table 1. Departments of the InVS.

	Number of tags	Number of persons	Coverage	Floor
DISQ	15	19	79%	0
DMCT	30	46	65%	0
DSE	38	60	63%	1
SRH	13	15	87%	1
SFLE	4	5	80%	0
Total	100	145	69%	

in departments determine the structure of the contact network and the dynamics of the contacts, and how these features affect epidemic spreading. We then focus on a new way to determine important nodes in such a contact network, based on the fraction of links each individual has with other individuals in the same department and in other departments, and present numerical simulations of an agent-based model of disease spread in order to discuss the efficiency of vaccination strategies based on this criterion.

2 Data collection

In order to collect data on the contacts between individuals, we used the sensing platform developed by the SocioPatterns¹ collaboration, based on wearable sensors that exchange ultra-low power radio packets in order to detect close proximity of individuals wearing them (Cattuto et al., 2010; Barrat et al., 2014). Each individual that accepted to participate in the study was asked to wear a sensor on his/her chest. As described elsewhere (Cattuto et al., 2010; Barrat et al., 2014), the body acts as a shield at the radio frequencies used by the sensors, so that the sensors of two individuals can only exchange radio packets when the persons are facing each other at close range ($\lesssim 1.5$ m). Signal detection is set so that any contact that lasts at least 20 seconds is recorded with a probability higher than 99 % (Cattuto et al., 2010). This defines the time resolution of the setup.

The study took place in one of the two office buildings of the InVS, located in Saint Maurice near Paris, France, and lasted two weeks. The building hosts three scientific departments—the *Direction Scientifique et de la Qualité* (DISQ, Scientific Direction), the *Département des Maladies Chroniques et des Traumatismes* (DMCT, Department of Chronic Diseases and Traumatisms) and the *Département Santé et Environnement* (DSE, Department of Health and Environment)—along with Human Resources (SRH) and Logistics (SFLE). DSE and DMCT are the largest departments, with more than 30 persons each, DISQ and SRH consist of around 15 persons, and finally logistics consists of only 5 persons (Table 1). DISQ, DMCT, and SFLE share the ground floor, while DSE and SRH are located on the first floor.

Two-thirds of the total staff agreed to participate to the data collection. The coverage ranges from 63% (DSE, the largest scientific department) to 87 % (human resources) (see Table 1). A signed informed consent was obtained for each participating individual and the French national bodies responsible for ethics and privacy, the

¹ <http://www.sociopatterns.org/>

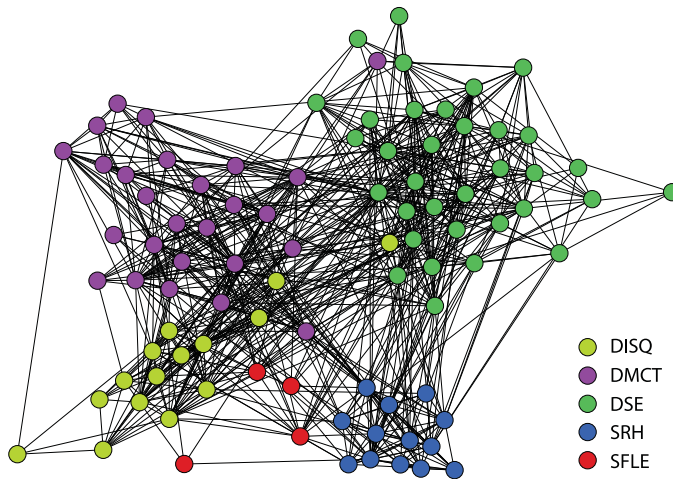


Fig. 1. Empirical network of contacts between individuals, aggregated over the two weeks of study. Each node represents an individual and the color-code corresponds to the different departments. Each link between two nodes indicates that the corresponding individuals have been in contact at least once during the data collection. Nodes are laid out using the Force Atlas algorithm (see Gephi software, <http://www.gephi.org>), which allows communities to be apparent in the visualization of the network. (Color online)

Commission Nationale de l'Informatique et des Libertés (CNIL, <http://www.cnil.fr>) was notified of the study. Data were treated anonymously, and the only information associated with the unique identifier of each sensor was the department of the individual wearing it.

3 Contact dynamics

3.1 Aggregated and temporal contact networks

We build the global contact network, shown in Figure 1, by aggregating the contact data over the two weeks of the experiment. Each node represents an individual, and a link is drawn between two nodes if the corresponding individuals have been in contact at least once during the study. Each link carries a weight calculated as the total duration of the contacts between the two individuals. The resulting distributions of node degrees (the degree of an individual gives the total number of distinct other individuals with whom (s)he has been in contact during the study) and link weights are shown in Figure 2(a) and (b). Moreover, we take advantage of the fact that the data is time-resolved to treat the contact network as a temporal network (Holme & Saramäki, 2012) and compute the distributions of contact durations and of the times between successive contacts of an individual (Figure 2(c) and (d)).

In addition to the statistics of the present data set, Figure 2 also displays the properties of networks of face-to-face contacts collected in two other settings, namely a conference (Stehlé et al., 2011b) and a high-school (Fournet & Barrat, 2014). Although the contexts are very different, the distributions are extremely similar. In particular, we find broad distributions with an approximate power-law shape for weights, contact, and inter-contact times, which are typical of the heterogeneous behavior often found in human activities (Barabási, 2005).

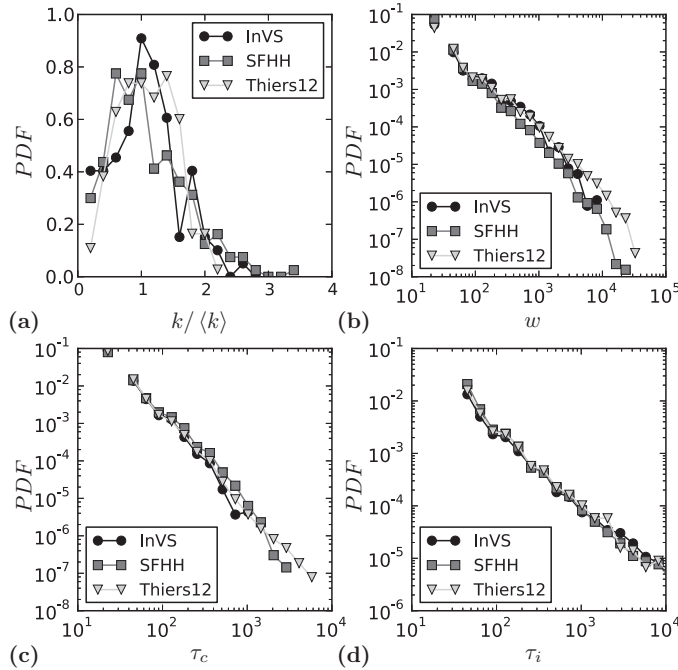


Fig. 2. Main features of the contact data. For each distribution we compare the features of the present study (InVS) with two previous studies: a scientific conference (SFHH, cf. (Stehlé et al., 2011b)) and a high school (Thiers12, cf. (Fournet & Barrat, 2014)). (a) Distributions of normalized degrees. Original mean degrees are: 15.1 (InVS), 47.5 (SFHH), 26.4 (Thiers12). (b) Link weight distributions. (c) Contact time distributions. (d) Inter-contact time distributions.

3.2 Sparsity of the contacts and consequences for the potential spread of infectious diseases

One of the main specific features of the present data set is the sparseness of the contacts: although the study lasted two weeks, the average degree in the aggregated network is only around 15, meaning that each individual met only $\sim 15\%$ of the office population participating to the study over the course of these two weeks. The contact network is thus very far from a fully connected structure, with immediate consequences on possible dynamical processes taking place on such a network, such as the propagation of an infectious disease.

To explore this issue, we perform numerical simulations of the spread of a Susceptible-Infected-Recovered (SIR) epidemic model in the population under study. In this model, Susceptible nodes (S) are infected with rate β when they are in contact with an infected node (I): for each small time step dt , an S node in contact with n I nodes becomes infected with probability $n\beta dt$. Infected nodes (I) recover from the infection with rate μ and enter the Recovered (R) compartment. Recovered nodes cannot be infected again. Our goal here is not to explore the whole phase diagram of the spreading process but rather to illustrate the influence of the contact patterns and of the interplay between the time-scales of the contacts and of the spreading process. We therefore consider two different values of the ratio β/μ and vary the speed of the epidemics by changing β . We vary β in order to explore a wide range

of time-scales: $\beta \in [0.0004; 0.02]$, which correspond to a typical time of infection $\beta^{-1} \in [50, 2, 500]$ seconds; For $\beta/\mu = 100$, we thus have $\mu^{-1} \in [1.4; 70]$ hours, and for $\beta/\mu = 1000$, $\mu^{-1} \in [14; 700]$ hours. The duration of the spread depends on the value of β and ranges from 10^5 to 10^7 seconds.

Each simulation starts with a single, randomly chosen, infected node (“seed”). We use the time-resolved data set to recreate *in-silico* the contacts between individuals (including the periods of inactivity, i.e., nights and week-end, during which individuals are considered isolated) and thereby the possibility of the infection to spread. We run each simulation until no infected individual remains (nodes are thus either still S or have been infected and have then recovered (R)). We define the duration T of an epidemic as the time needed to reach this state, and the final size N of an epidemic as the number of nodes that have been affected by the spread, i.e. the number of R nodes at the end of the epidemic. As T might be longer than the duration of the data set, we repeat the two-weeks sequence of contacts in the simulation if needed (Stehlé et al., 2011b). For each realization we randomly choose both the seed and the moment when the spreading process starts. We compute the statistics of the final epidemic size over 1,000 realizations for each value of the parameters.

Figure 3 displays the resulting distributions (i.e., the probability that the spread affects N individuals). For $\beta/\mu = 100$, no large outbreaks are obtained (Figure 3(a)). Even for the longest values of the infectious period (lowest values of μ), the sparsity of contacts makes the propagation of infection difficult. Indeed, at the fastest time scale, i.e., the time resolution of 20 seconds, nodes have an average instantaneous degree of 0.013, and overall only 0.66 links exist on average in the whole network: very few transmission opportunities exist at each time. Epidemics spread only if the ratio β/μ is increased enough to compensate for this very low contact rate (e.g., if, at fixed β , the recovery rate is strongly decreased). An example is given in Figure 3(b) where we use $\beta/\mu = 1,000$. Even in this case, many realizations lead to epidemics of small size, but epidemics affecting a large fraction of the population are also obtained.

Interestingly, Figure 3(b) also illustrates the role of the interplay between the timescale of the disease spread and of the contact network (Isella et al., 2011b; Barrat et al., 2013). At fixed β/μ indeed, a mode of the distribution corresponding to large epidemics is present for small values of β and μ . Larger values of β and μ corresponding to faster processes, with high spreading probability at each contact but also fast recovery and thus shorter infectious periods, lead to smaller probabilities of large epidemics: as β is increased, the mode of the distribution corresponding to large epidemics tends to be suppressed. This phenomenon is related to the temporal constraints and correlations inherent in temporal networks that can slow down and hamper the propagation of rapidly spreading processes (Karsai et al., 2011; Isella et al., 2011b; Pfitzner et al., 2013; Scholtes et al., 2014): for instance, if A meets B who is infectious, and then C , the infection can spread from B to C through A . If instead A meets first C then B , A cannot be an intermediary for the spread to C . Slowly spreading processes—with slow recovery—on the other hand are “less constrained” as the infectious period is longer and contacts with more individuals or repeated contacts with the same individual can occur during this period, effectively creating more possible paths of transmission between individuals (Stehlé et al., 2011b; Holme & Saramäki, 2012; Barrat et al., 2013). To make the role of the

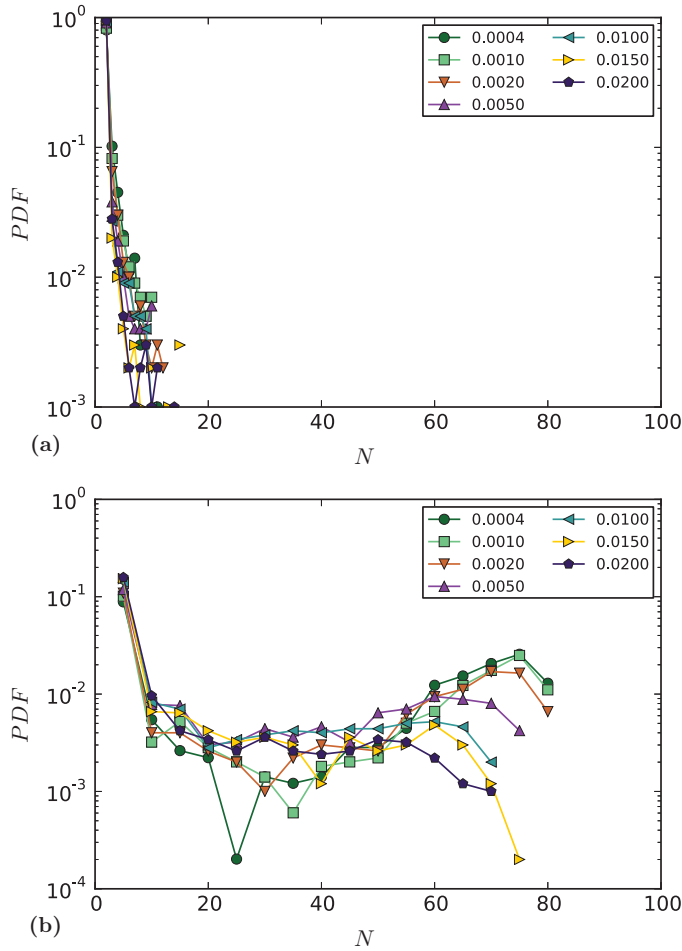


Fig. 3. Distributions of the final size N of simulated epidemics. Simulations are performed for different values of the infection rate β (given in the legend), the recovery rate μ being determined by the fixed β/μ ratio. At given β/μ , larger values of β correspond to both faster spread and faster recovery. For each value of β , distributions are computed from 1,000 simulations with initial conditions given by one single randomly chosen infected individual. (a) $\beta/\mu = 100$. (b) $\beta/\mu = 1,000$. (Color online)

contact chronology and of temporal constraints more explicit, we compare in the supplementary material the outcome of spreading processes simulated either on the temporally resolved contact data or on aggregated versions of the data, in which the information about the order in which different contacts occur is lost. Spreading processes with fixed β/μ values unfolding on a purely static contact structure would lead to exactly the same distribution of final epidemic sizes for different values of β . In our case, we still take into account the fact that nodes are isolated during nights and weekends. As a result, larger values of β lead to slightly larger epidemics, because faster spreading processes unfold over less inactivity periods (and inactivity periods, during which nodes can recover but cannot transmit, tend to hinder the spread). Overall, we thus have an opposite trend on temporal and static networks, at fixed β/μ : on static networks, increasing β tends to increase the final epidemic size

and, in particular, the mode at large final sizes is kept, while if the whole temporal resolution is considered, such an increase tends to suppress the large epidemics.

3.3 Organization in departments

The offices are organized in five departments, on two floors. DISQ, DMCT, and SFLE (logistics) are on the ground floor, along with a cafeteria and conference rooms. The remaining departments—SRH (human resources) and the DSE department—are on the first floor. As found in the literature linked to social sciences and architecture, the spatial organization is expected to have an impact on the interactions between office workers (Penn et al., 1999; Sailer & McCulloh, 2012; Brown et al., 2014b; Brown et al., 2014a). A detailed investigation of this issue is beyond the scope of our work, in particular as, due to anonymity of the participants, we do not have access to the office location of each participant. As shown in Figure 1 the collected data show nonetheless a clear impact of the structure in departments, while the separation in two different floors is less apparent, at least at this resolution. As we will see in the next sections and as discussed for instance in (Salathé & Jones, 2010; Hébert-Dufresne et al., 2013), the fact that departments seem to correspond to communities in the network structure shown in Figure 1 has consequences for the possibility to define mitigation strategies against the spread of epidemics.

In order to better quantify the mixing within and between departments, we build contact matrices giving for each pair of departments the total time of contact between individuals belonging to these departments. Figure 4(a) shows that contacts occur much more often inside departments (internal contacts) than between them (external contacts), with the exception of the logistics department. Furthermore, it confirms that the structure of external contacts does not clearly follow the spatial organization in two floors, but that scientific departments form a moderately connected substructure, leaving human resources and logistics more isolated. This structure is also found in the contact matrix restricted to the conference rooms (Figure 4(b)). Scientific departments are in fact almost the only ones using these rooms for inter-departments meetings. Contacts between individuals of different departments also occur independently of scheduled meetings, for instance during lunch, which takes place either in the cafeteria or in the canteen (located in a distinct building). The contacts taking place in the cafeteria at lunchtime (Figure 4(c)) show the same structure as the global one, with many internal contacts for each department, and a substructure corresponding to the three scientific departments on the one hand, and logistics and human resources on the other hand. Strikingly, the structure of contacts occurring in the canteen is rather different, with a mostly diagonal contact matrix: in this situation, individuals from different departments do not mix with each other. In order to test if such structures of contact patterns can simply be explained by the fact that the departments are of different sizes or that individuals from the same department tend to be present at a given location at the same time, we consider in the electronic supplementary material a null model in which contacts occur at random between nodes that are present in the same location at the same time, according to their empirical presence timeline and with a constant rate set to yield the same total contact time as in the empirical data. The empirical contact matrices are significantly different from the ones obtained with such a null model,

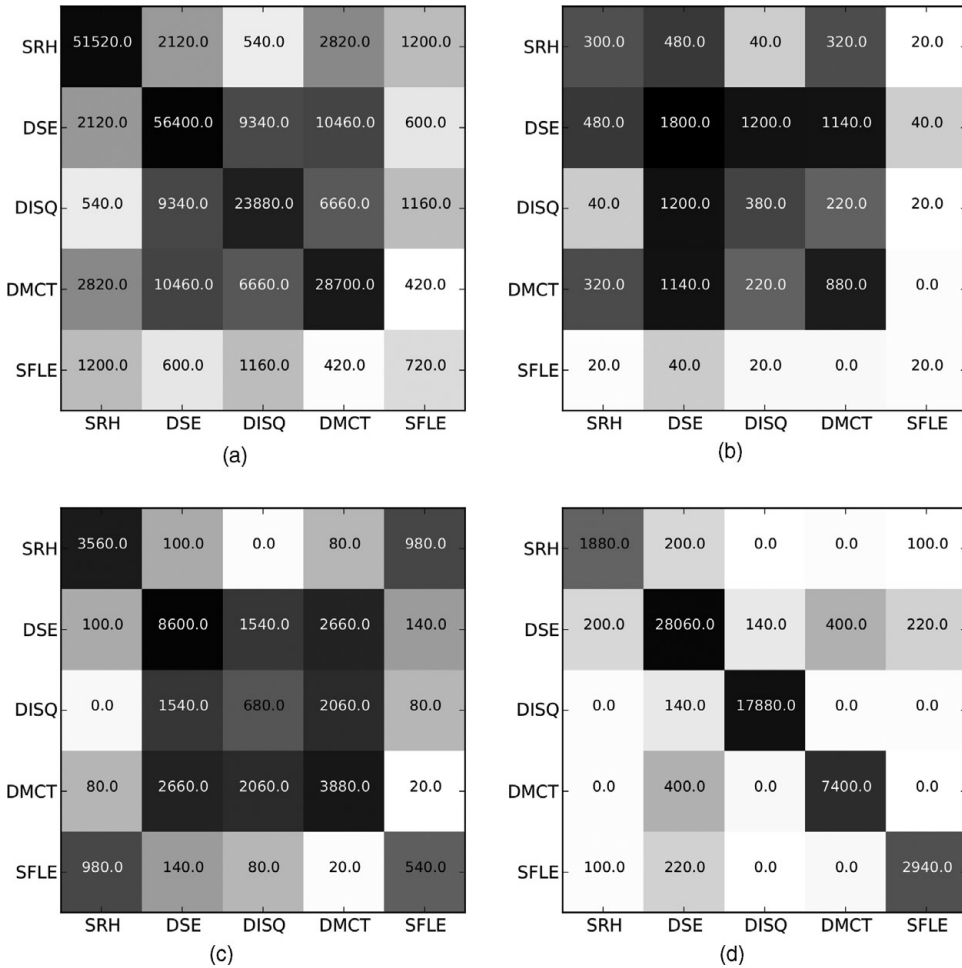


Fig. 4. Contact matrices. Each matrix element (at row X and column Y) gives the total time of contact between individuals from departments X and Y during the two weeks of the study, in different locations. (a) Entire building. (b) Conference room. (c) Cafeteria, restricted to the interval between 12 am and 2 pm for each day. (d) Canteen. This place is in a different building and is not taken into account in (a).

showing that the observed structure is indeed the result of individual choices and non-random interactions.

Overall, the structure of contacts measured in the InVS offices is strongly shaped by its internal organization in departments. Although contacts are *a priori* not constrained by specific schedules, as e.g., in schools or high schools (Stehlé et al., 2011a; Fournet & Barrat, 2014), the resulting patterns are still very different from contexts such as conferences (Stehlé et al., 2011b), and in particular very far from a homogeneous mixing situation. This has clear consequences in the design of realistic agent-based models of workplaces. For instance, as shown in the electronic supplementary material, modeling the spread of a disease in such a context under a homogeneous mixing assumption would result in a lack of accuracy with respect to more realistic data representations which take into account the division in departments and the restricted mixing between departments.

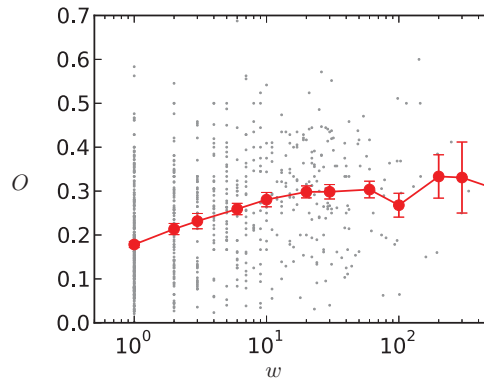


Fig. 5. Overlap of a link as a function of its weight. Scatter plot (gray) is averaged on weight bins (red). The error bars mark the standard error on the average value. (Color online)

3.4 Weak inter-department ties

We investigate in more detail how the network structure is shaped by the departments by computing, as suggested in (Onnela et al., 2007), the topological overlap O_{ij} of the neighborhoods of each pair of connected nodes i and j : $O_{ij} = n_{ij} / ((k_i - 1) + (k_j - 1) - n_{ij})$, where k_i and k_j are the respective degrees of i and j and n_{ij} is the number of common neighbors of i and j . If $O = 0$ the two nodes do not share any neighbors, while if $O = 1$ the two nodes have exactly the same neighbors. The topological overlap thus quantifies whether a link joins two nodes from the same group or community in the network, or two nodes from different communities. Figure 5 shows, similarly to the results of (Onnela et al., 2007) concerning a communication network, that overlaps and weights are positively correlated (we recall that the weight of a link is the total contact time between the two linked individuals). Moreover, we measure for internal links an average overlap of 0.29, with an average weight of 328 s, while links joining individuals from different departments have an average overlap of 0.13 and an average weight of 134 s. This indicates that internal links are strong, whereas external links tend to be the weak ties in agreement with the *weak tie hypothesis* of Granovetter (1973).

3.5 Daily contacts structure

3.5.1 Stability of the overall structure

In order to understand how well the structure of the globally aggregated contact network and of the contact matrices described in the previous paragraph reflect how contacts occur every day, we build contact matrices giving for each day the durations of contacts between individuals of different departments (shown in the electronic supplementary material) and compare their properties. Table 2 presents the mean similarity between each daily contact matrix and the matrices of the other days. The high values obtained show that the structure of the contact matrix is largely conserved from one day to another. As the diagonal of the matrices contains the largest values, we also compute similarities restricted to the non-diagonal elements.

Table 2. Daily contact matrices similarities. For each day, we compute the cosine similarity between the list of elements of the contact matrix and the ones of the other days, both with and without the diagonal elements. We list in this table the mean value and the standard deviation of the similarities.

Day	Full	w/o diagonal
06/24	0.753 ± 0.103	0.563 ± 0.222
06/25	0.843 ± 0.069	0.481 ± 0.087
06/26	0.837 ± 0.046	0.400 ± 0.246
06/27	0.870 ± 0.052	0.534 ± 0.108
06/28	0.871 ± 0.075	0.426 ± 0.134
07/01	0.821 ± 0.058	0.592 ± 0.152
07/02	0.850 ± 0.087	0.579 ± 0.180
07/03	0.858 ± 0.072	0.488 ± 0.262
07/04	0.767 ± 0.058	0.317 ± 0.131
07/05	0.795 ± 0.123	0.398 ± 0.199

We still obtain rather large values, showing that even secondary structures are stable across days.

3.5.2 Network evolution

Although the overall contact structure is rather stable from one day to the next, the specific contacts of each individual change. Indeed, Figure 6(a) shows that the average degree (number of distinct individuals contacted) of individuals increases steadily when we consider contact networks aggregated over increasing time intervals, both within a department and for external contacts. In order to gain more insights into this issue, we compute similarities between daily aggregated contact networks: the similarity between two networks (1) and (2) is defined here as the cosine similarity between their weighted lists of links, $\sum_{i,j} w_{ij,(1)} w_{ij,(2)} / \sqrt{\sum_{i,j} w_{ij,(1)}^2 \sum_{i,j} w_{ij,(2)}^2}$ where $w_{ij,(a)}$ is the weight of the link ij in network (a) (if there is no link, the weight is set equal to 0). The resulting values are given in Table 3(a).

In order to understand if these values correspond to a weak or strong stability, we compare them with several null models obtained by link rewiring. If we consider networks with the same number of nodes and the same set of weights, but edges placed at random between nodes (Table 3(b)), similarities are much smaller than for the empirical data. This is also the case if links are reshuffled while conserving the degree of each node (Maslov & Sneppen, 2002) (Table 3(c)) and if weights are redistributed at random among the links while conserving the topology of the networks (Table 3(d)). Finally, even null models which respect the department structure, i.e., with rewiring or reshuffling procedures inside each compartment of the contact matrix, yield similarities smaller than the empirical ones (Table 3(e) and (f)).

Overall, these results indicate on the one hand that the precise structure of the daily contact networks fluctuates significantly across days, even if the contact matrix structure is stable. On the other hand, the changes from one day to the next are much less important than what would be obtained by random chance, and even some degree of intra-department structure is kept across days. Such results should

Table 3. Daily networks similarities. For each day, we calculate the cosine similarity between the weighted link list of the corresponding network and the lists of all other days. We show here the mean and standard deviation of these similarities. Statistics for the null models are calculated over 1,000 realizations. (a) Empirical similarities. (b) Complete random rewiring of links. (c) Rewiring keeping each individual node degree fixed. (d) Random redistribution of link weights on the fixed topological structure. (e) Rewiring in each contact matrix compartment. (f) Random redistribution of link weights in each contact matrix compartment.

Day	(a)	(b) ($\times 10^{-3}$)	(c) ($\times 10^{-2}$)	(d) ($\times 10^{-2}$)	(e) ($\times 10^{-2}$)	(f) ($\times 10^{-2}$)
06/24	0.141 ± 0.084	6.20 ± 13.8	1.51 ± 1.56	3.83 ± 3.50	2.19 ± 2.69	4.39 ± 3.63
06/25	0.302 ± 0.162	5.30 ± 13.5	2.40 ± 4.46	4.07 ± 3.90	3.56 ± 5.41	6.34 ± 6.59
06/26	0.125 ± 0.052	5.33 ± 15.6	2.29 ± 3.44	3.96 ± 3.99	2.90 ± 3.75	5.15 ± 4.78
06/27	0.288 ± 0.195	6.32 ± 14.8	2.01 ± 2.09	4.67 ± 3.65	3.48 ± 4.73	6.27 ± 6.10
06/28	0.096 ± 0.041	5.30 ± 12.8	2.23 ± 3.43	4.98 ± 4.08	4.01 ± 5.38	7.55 ± 6.55
07/01	0.109 ± 0.078	4.15 ± 11.9	1.67 ± 2.93	4.07 ± 4.08	2.19 ± 2.35	4.75 ± 3.65
07/02	0.264 ± 0.141	5.85 ± 14.7	2.65 ± 3.92	5.28 ± 4.10	4.36 ± 4.76	8.06 ± 5.83
07/03	0.318 ± 0.206	5.23 ± 14.3	2.03 ± 2.35	4.56 ± 4.04	3.36 ± 5.22	6.72 ± 7.07
07/04	0.246 ± 0.101	5.03 ± 13.9	1.62 ± 2.19	3.94 ± 3.90	2.46 ± 3.22	5.23 ± 4.64
07/04	0.297 ± 0.262	2.52 ± 11.4	1.37 ± 4.11	2.43 ± 3.96	2.75 ± 6.37	4.79 ± 8.05

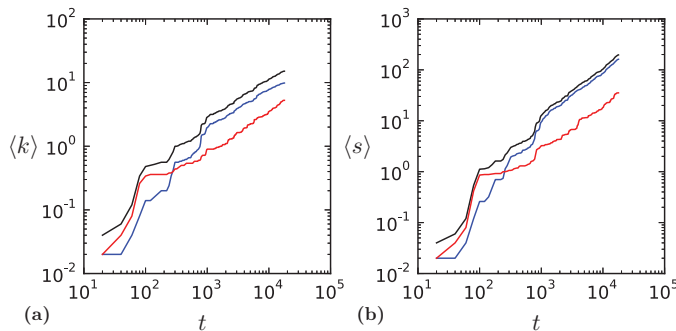


Fig. 6. Network aggregation. We compute the mean degree (number of distinct individuals contacted) (a) and the mean node strength (total time in contact) (b) as a function of time while aggregating the network over the two weeks of measurement, disregarding nights and the weekend. These are calculated globally (black), and restricted to internal links (blue) and external links (red). (Color online)

thus be taken into account in the development of agent-based models, as done e.g., in (Stehlé et al., 2011b), as the amount of repetition of contacts over different days impacts how dynamical processes such as epidemics unfold in a population (Smieszek et al., 2009).

3.5.3 Daily activity

As Figure 6(b) shows, the total duration of contacts within and between departments grows steadily. Contacts however might *a priori* occur at specific times for specific departments (due to breaks, meetings, etc. . .). We therefore examine in Figure 7 the activity timelines averaged over different days. The global, averaged activity for the whole building (Figure 7(a)) exhibits activity peaks around 10 am and lunchtime,

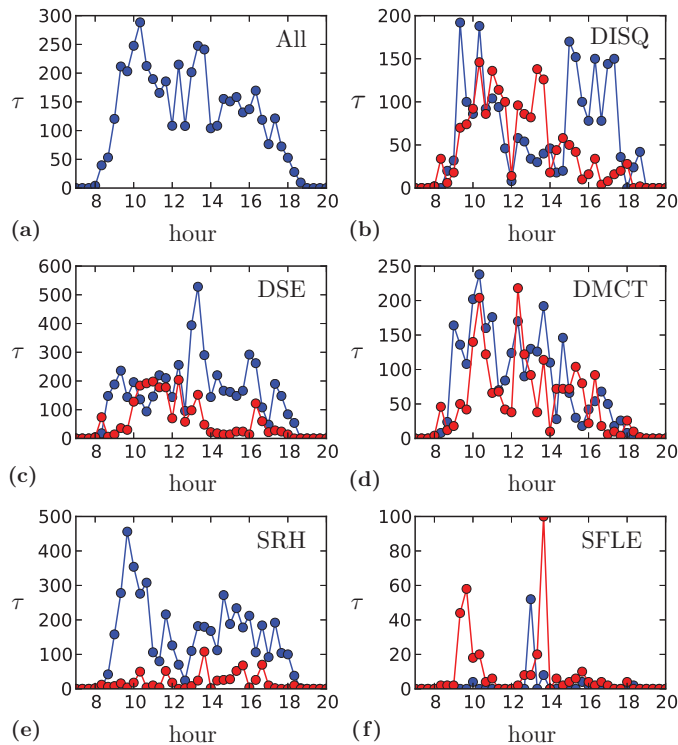


Fig. 7. Daily activity timelines for each department. The activity is defined as the total duration of contacts during windows of 20 minutes. We show the activity averaged over the ten days of the study. Internal contacts are plotted in blue, external contacts in red. (Color online)

but no other clear feature emerges. This is most probably due to the fact that no strict schedule constraints exist (in contrast e.g., to schools (Stehlé et al., 2011a) and hospitals (Vanhems et al., 2013)). We also show for each department both internal and external contact activities for an average day (Figure 7(b)–(f)). Four departments present the 10 am peak of activity, which may be related to a common tendency to have a break around that time. During lunch (12 am–2 pm), DSE, DMCT, and SFLE have many contacts, both within and outside the department, whereas SRH exhibits a decrease of activity, and DISQ shows an inversion between internal and external contacts. Finally, for the three scientific departments, external contacts are more present in the morning than in the afternoon.

4 Node behaviors

4.1 Residents, wanderers and linkers

In the context of spreading phenomena, links joining groups of individuals in a contact network play a crucial role (Karsai et al., 2011; Onnela et al., 2007; Salathé & Jones, 2010; Hébert-Dufresne et al., 2013). In the present case, the possibility for an infectious disease to spread in the whole population thus strongly depends on the structure of contacts along inter-departments links. In order to shed more light on the role of each node in linking communities, we consider the static aggregated network, and we compute in Figure 8 for each node the fraction of its links with

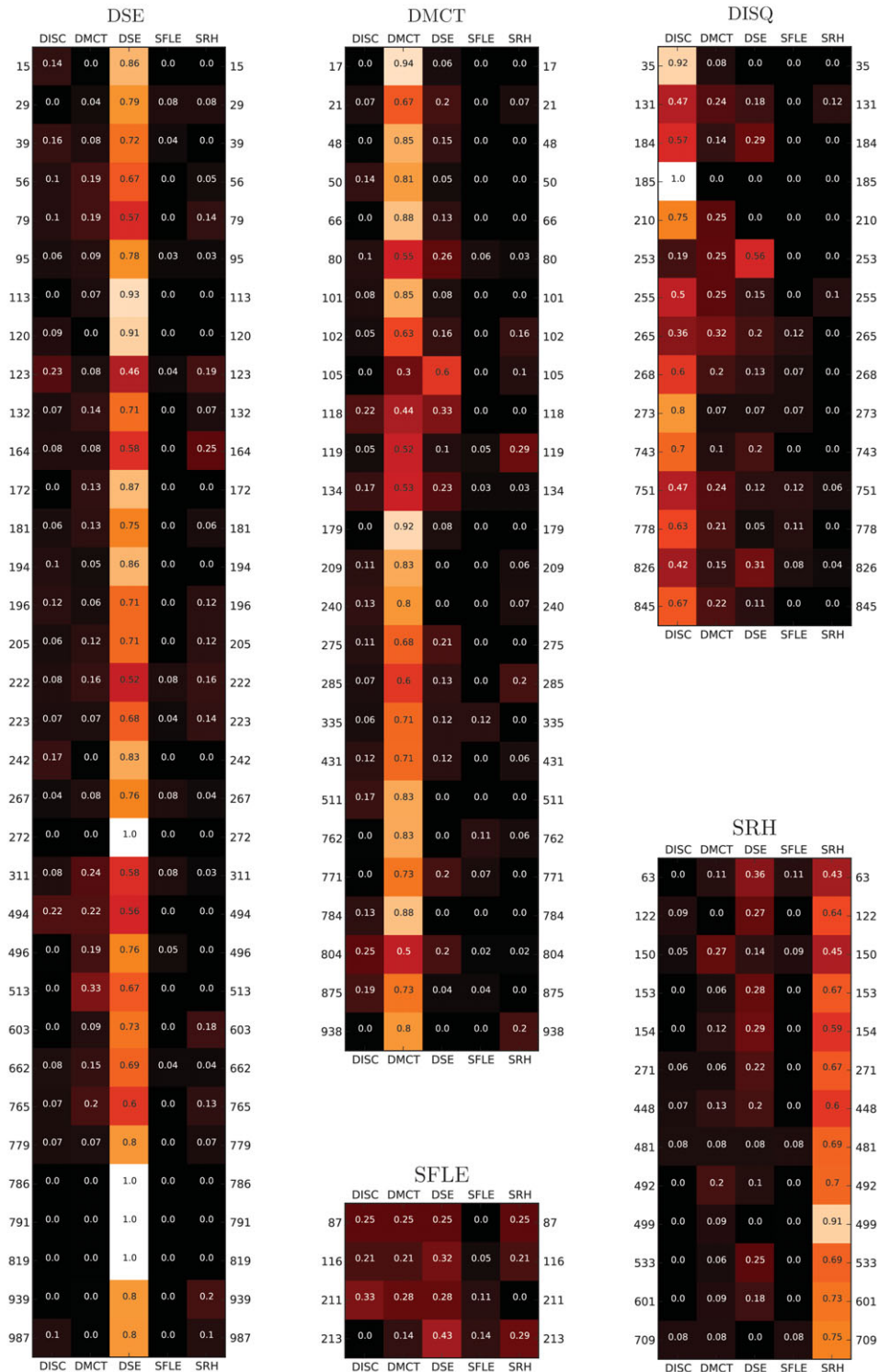


Fig. 8. Proportion of links with individuals of each department, for each node. Values are calculated from the network aggregated over the two weeks. (Color online)

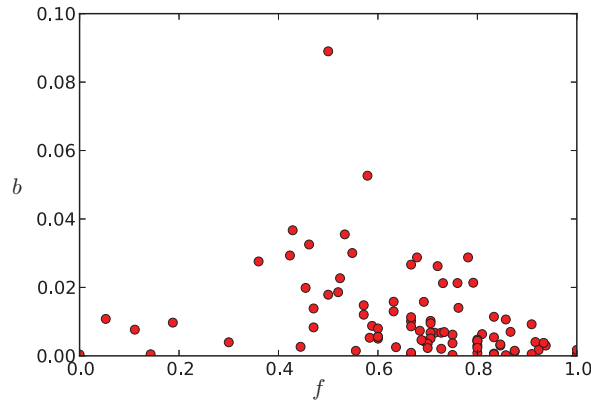


Fig. 9. Relation between the betweenness centrality b of a node and the fraction f of its links that are internal. Values are calculated on the network aggregated over the two weeks. (Color online)

individuals of each department. We focus in particular on the fraction f of internal links (i.e., with nodes in the same department). Most nodes are “residents”: the large majority of their links are internal. Some other nodes (such as individuals from the Logistics department, or node 105 from DMCT and node 253 from DISQ) are on the other hand, mostly linked to nodes outside their own department: they are “wanderers.”

In order to determine how these different types of behavior could be exploited in the design of targeted vaccination strategies, we investigate in Figure 9 the relation between the centrality of a node in the aggregated contact network, as measured by its betweenness centrality (BC), and its fraction f of internal links. We note here that different definitions of node centrality exist. They are often correlated but the precise ranking of nodes’ centrality slightly depends on the specific centrality measure used, and various works have compared how different centrality measures perform in identifying individuals most at risk of infection or the most efficient spreaders for various models of epidemic spreading (Christley et al., 2005; Kitsak et al., 2010; Castellano & Pastor-Satorras, 2012). In the context of targeted measures to mitigate the spread of diseases in particular, immunizing (i.e., removing) the nodes with highest degree or largest BC is known to be among the most efficient strategies (Pastor-Satorras & Vespignani, 2002; Holme et al., 2002; Dall’Asta et al., 2006). We also note that BC can be defined both on the unweighted and weighted versions of the network (Dall’Asta et al., 2006; Opsahl et al., 2010). We have considered both cases and found very similar results so we use for simplicity in Figure 9 the unweighted BC.

Residents have, as could be expected, low centrality. Wanderers, as nodes connecting to other departments, could be expected to be crucial in potential spreading paths. However, they turn out to have low centralities as well. The most central nodes correspond to a specific population, composed of nodes whose neighborhood is composed by approximately one half of internal links and one half of external links. We call them “linkers,” as they are effectively responsible for the connectivity between the departments and act as bridges (Wasserman & Faust, 1994) between them.

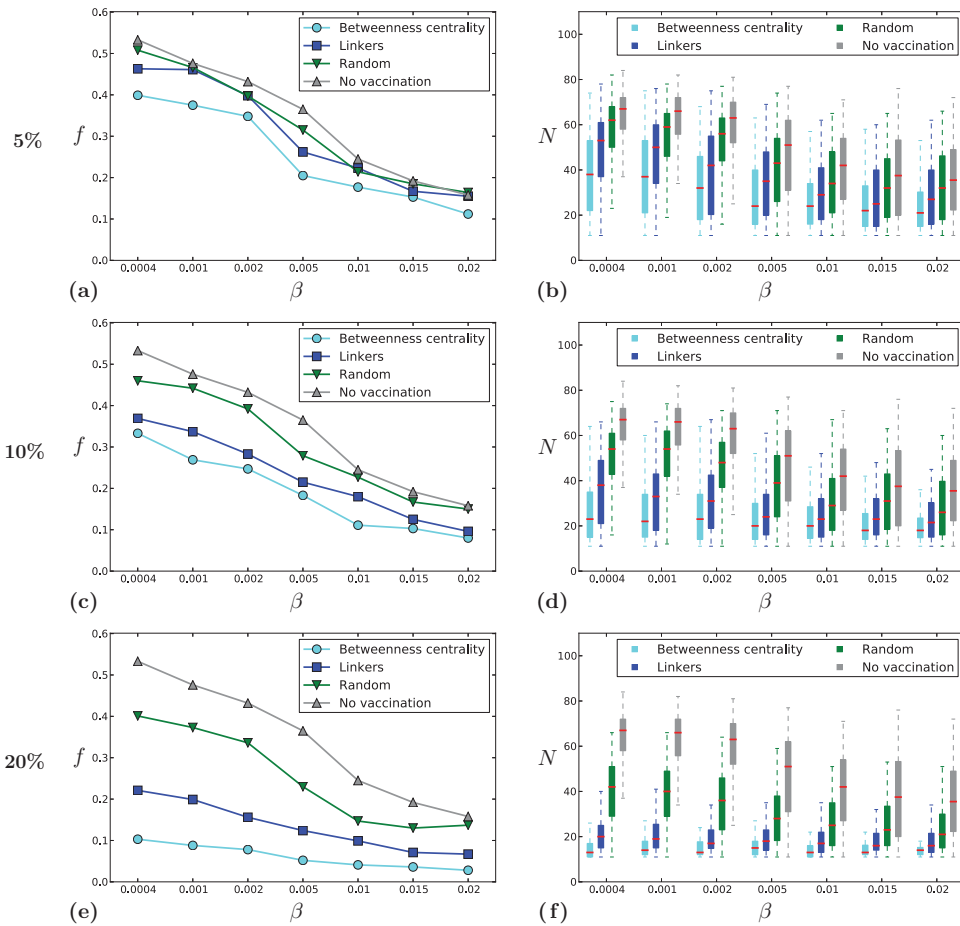


Fig. 10. Vaccination strategies. We simulate SIR epidemics on the time-resolved contact network, with $\beta/\mu = 1,000$, in order to test different vaccination strategies. In each case we perform 1,000 realizations. (a), (c), (e) Fraction f of epidemics that reach more than 10 individuals. (b), (d), (f) Size distribution of these large epidemics. For each strategy we vaccinate nodes according to the following rules: highest betweenness centralities, best linkers (fraction of internal links closest to 0.5) and random choice. We also plot the case without vaccination as a reference. (Color online)

4.2 Linkers and spreading processes

As the linker behavior seems to be associated with high node centralities in the aggregated contact network, we consider here the effect on a potential epidemic spread of a containment strategy targeting linkers. Although it is expected that the precise detection (and vaccination) of the nodes with the highest centrality would be more efficient, as the correlation between linkers and high centrality nodes is not perfect, the detection of linker behavior relies *a priori* on less information than the computation of betweenness centralities and might thus represent an interesting alternative. We show in Figure 10 the result of simulated SIR processes on the temporal contact network when a fraction of nodes are vaccinated, i.e., considered immune to infection (they can neither be infected nor transmit the infection), according to different strategies. The figure shows that the targeted vaccination of

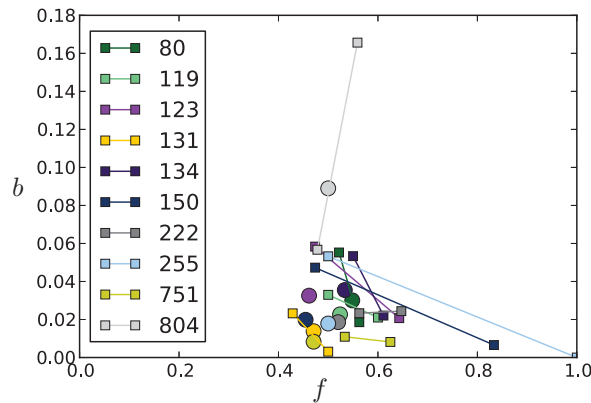


Fig. 11. Stability of linker behavior during the two weeks. For each node defined as a linker from the two weeks of data, we plot its characteristics based on each week's data (squares). Circles show their positions according to the full two weeks of data. (Color online)

linkers decreases the probability to observe a large outbreak, and, in the case of such an outbreak, limits its size. This strategy is much more efficient than random vaccination, and, for a vaccination rate of 20%, performs almost as well as a strategy based on centrality, with a strongly decreased outbreak probability. For a small vaccination rate (5%), the outbreak probability is not much reduced, but, in case of outbreak, the resulting epidemic sizes are clearly smaller than for a random vaccination strategy.

4.3 Stability of the linker behavior

Linkers are defined as nodes with approximately 50% external links, based on the network aggregated over the two weeks data set. If we perform the same analysis on data restricted to either of the weeks, we do not necessarily find the same nodes, as the fine structure of the networks fluctuates a lot from one day to another, as highlighted in the previous section. We investigate this point in Figure 11 by plotting, for each node with a linker behavior in the global two weeks aggregated networks, its BC versus its fraction of external links in each of the two networks aggregated over one week. Though some of these nodes would not be selected as linkers if we restricted the data to one week, their behavior can still be considered as linker-like, as the fraction of external links remains between 40 % and 60 % for most of them. Only two nodes (150 and 255) are insiders one week and linkers the other week. The linker behavior thus seem rather stable over time, and a one week data set may be enough to find linkers. To check this hypothesis, we perform simulations of an SIR model using data corresponding to one of the two weeks of the study, and use a vaccination strategy targeting the linkers defined using data from the other week. Figure 12 shows that, although this strategy performs less well than the strategy using linkers defined from the full two weeks data, it still largely outperforms random vaccination in reducing the risk of large outbreaks and the size of large epidemics. The reduced efficiency obtained when using data from one week to define a strategy applied in the other week is reminiscent of the results of

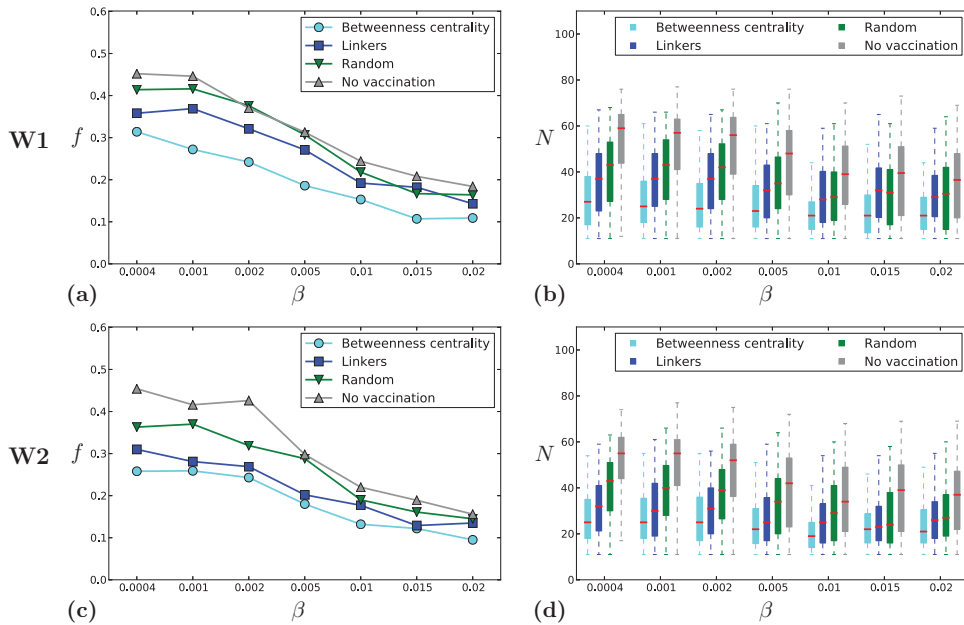


Fig. 12. Efficiency of sampling over one week. We simulate SIR epidemics on the temporal contact network, with $\beta/\mu = 1,000$, over only one week of data, with vaccination strategies based on data from the other week. In each case 10% of the population was vaccinated. The labels indicate on which week the vaccination strategies were defined. (Color online)

(Starnini et al., 2013) showing a limit in the efficiency of vaccination strategies due to the fluctuations of contact networks.

5 Discussion

In this paper, we analyzed data describing the contacts between individuals in the context of an office building. Not all individuals participated in the study, which means that the data cover only a part of the real contact network. As the sampled fraction is quite high, and uniform among the departments, we assume that the behavior of the sampled population is representative of the whole.

Under this caveat, we have shown that, in this situation, many statistical features of contacts are similar to the ones measured in different contexts, with some important specificities. First, contacts are very sparse, which for instance tends to hinder the spread of infectious diseases, especially rapidly spreading ones. Second, the contact network is structured in communities that approximately match the organization in departments of the building. The connections between departments do not reflect their spatial organization in the building, but rather their roles: the three scientific departments form a cluster, whereas human resources and logistics are more isolated. The structure is thus very different from a homogeneous mixing hypothesis, with important consequences on the design of agent-based models of e.g., epidemic spreading processes.

The presence of a strong community structure linked to the organization in departments in the contact network has led us to define three node behaviors, depending on the fraction of links each node shares within its own department:

residents, whose links are mostly internal; wanderers, whose links are mostly external; linkers, whose links are half internal, half external, and therefore connect departments, acting as bridges between communities (Wasserman & Faust, 1994; Salathé & Jones, 2010). Empirically, the most central nodes of the network turn out to be linkers. As a consequence, targeted vaccination strategies based on the linker criterion efficiently prevents epidemic outbreaks. This behavior is also stable enough on the scale of one week for such a strategy to remain efficient if based on fewer data.

The precise identification of linker behavior relies on the knowledge of the contact network. One could thus argue that it requires almost as much knowledge as the identification of the nodes with highest BC. However, the linker behavior, contrary to the BC criterion, may be more easily linked to recognizable human behavior or to individual attributes in the organizational chart, for instance in relation to professional grade or specific activities. In this case, one could *a priori* discern which individuals are more susceptible to be linkers and play an important role in the event of an outbreak, and therefore use such limited information to design an efficient vaccination strategy entailing only a low cost in terms of necessary information (Smieszek & Salathé, 2013; Chowell & Viboud, 2013). We final note that the linker behavior might also be identified from limited information in other social contexts with communities—schools, hospitals, etc—and provide an important ingredient in agent-based models of epidemic spreading phenomena, as such agents provide crucial gateways between communities. Moreover, in the perspective of modeling and studying epidemic processes in real, large-scale systems, obtaining a complete data set of contacts between individuals in a large-scale population seems beyond reach, so that this type of criterion could be a way to uncover the central elements who could be targeted for outbreak detection and control.

Acknowledgments

We thank the direction of the InVS for accepting to host this study in their facility, and all the participants to the study. We acknowledge the SocioPatterns² collaboration for providing the sensing platform that was used in the collection of the contact data. M.G., I.B. and A.B. are partially supported by the French ANR project HarMS-flu (ANR-12-MONU-0018); C.L.V. and A.B. are partially supported by the EU FET project Multiplex 317532.

Supplementary material

To view supplementary material for this article, please visit <http://dx.doi.org/10.1017/nws.2015.10>

References

- Ajelli, M., Gonçalves, B., Balcan, D., Colizza, V., Hu, H., Ramasco, J., ... Vespignani, A. (2010). Comparing large-scale computational approaches to epidemic modeling: Agent-based versus structured metapopulation models. *BMC Infectious Diseases*, **10**(1), 190.

² <http://www.sociopatterns.org/>

- Ajelli, M., Poletti, P., Melegaro, A., & Merler, S. (2014). The role of different social contexts in shaping influenza transmission during the 2009 pandemic. *Scientific Reports*, **4**, 7218.
- Barabási, A.-L. (2005). The origin of bursts and heavy tails in human dynamics. *Nature*, **435**, 207.
- Barrat, A., Cattuto, C., Colizza, V., Gesualdo, F., Isella, L., Pandolfi, E., . . . Broeck, W. (2013). Empirical temporal networks of face-to-face human interactions. *The European Physical Journal Special Topics*, **222**(6), 1295–1309.
- Barrat, A., Cattuto, C., Tozzi, A. E., Vanhems, P., & Voirin, N. (2014). Measuring contact patterns with wearable sensors: Methods, data characteristics and applications to data-driven simulations of infectious diseases. *Clinical Microbiology and Infections*, **20**(1), 10–16.
- Blower, S., & Go, M.-H. (2011). The importance of including dynamic social networks when modeling epidemics of airborne infections: Does increasing complexity increase accuracy? *BMC Medicine*, **9**(1), 88.
- Brown, C., Efstratiou, C., Leontiadis, I., Quercia, D., & Mascolo, C. (2014b). Tracking serendipitous interactions: How individual cultures shape the office. In *Proceedings of the 17th ACM Conference on Computer Supported Cooperative Work & #38; Social Computing*. CSCW '14. New York, NY, USA: ACM, pp. 1072–1081.
- Brown, C., Efstratiou, C., Leontiadis, I., Quercia, D., Mascolo, C., Scott, J., & Key, P. (2014a). The architecture of innovation: Tracking face-to-face interactions with ubicomp technologies. In *Proceedings of the 2014 ACM International Joint Conference on Pervasive and Ubiquitous Computing*. UbiComp'14. New York, NY, USA: ACM, pp. 811–822.
- Castellano, C., & Pastor-Satorras, R. (2012). Competing activation mechanisms in epidemics on networks. *Scientific Reports*, **2**, 371.
- Cattuto, C., Van den Broeck, W., Barrat, A., Colizza, V., Pinton, J.-F., & Vespignani, A. (2010). Dynamics of person-to-person interactions from distributed RFID sensor networks. *PLoS ONE*, **5**(7), e11596.
- Chowell, G., & Viboud, C. (2013). A practical method to target individuals for outbreak detection and control. *BMC Medicine*, **11**(1), 36.
- Christley, R. M., Pinchbeck, G. L., Bowers, R. G., Clancy, D., French, N. P., Bennett, R., & Turner, J. (2005). Infection in social networks: Using network analysis to identify high-risk individuals. *American Journal of Epidemiology*, **162**(10), 1024–1031.
- Dall'Asta, L., Barrat, A., Barthélemy, M., & Vespignani, A. (2006). Vulnerability of weighted networks. *Journal of Statistical Mechanics: Theory and Experiment*, **2006**(04), P04006.
- Davey, V. J., Glass, R. t J., Min, H. J., Beyeler, W. E., & Glass, L. M. (2008). Effective, robust design of community mitigation for pandemic influenza: A systematic examination of proposed US guidance. *PLoS ONE*, **3**(7).
- Eagle, N., Pentland, A. (Sandy), & Lazer, D. (2009). Inferring friendship network structure by using mobile phone data. *Proceedings of the National Academy of Sciences*, **106**(36), 15274–15278.
- Fournet, J., & Barrat, A. (2014). Contact patterns among high school students. *PLoS ONE*, **9**(9), e107878.
- Gauvin, L., Panisson, A., & Cattuto, C. (2014). Detecting the community structure and activity patterns of temporal networks: A non-negative tensor factorization approach. *Plos One*, **9**(1), e86028.
- Gauvin, L., Panisson, A., Cattuto, C., & Barrat, A. (2013). Activity clocks: Spreading dynamics on temporal networks of human contact. *Scientific Reports*, **3**, 3099.
- Gemmetto, V., Barrat, A., & Cattuto, C. (2014). Mitigation of infectious disease at school: Targeted class closure vs school closure. *BMC Infectious Diseases*, **14**(1), 695.
- Granovetter, M. (1973). The strength of weak ties. *American Journal of Sociology*, **78**, 1360–1380.

- Hébert-Dufresne, L., Allard, A., Young, J.-G., & Dubé, L. J. (2013). Global efficiency of local immunization on complex networks. *Scientific Reports*, **3**, 2171.
- Holme, P., Kim, B. J., Yoon, C. N., & Han, S. K. (2002). Attack vulnerability of complex networks. *Physical Review E*, **65**(May), 056109.
- Holme, P., & Saramäki, J. (2012). Temporal networks. *Physics Reports*, **519**(3), 97–125.
- Isella, L., Romano, M., Barrat, A., Cattuto, C., Colizza, V., Van den Broeck, W., . . . Tozzi, A. E. (2011a). Close encounters in a pediatric ward: Measuring face-to-face proximity and mixing patterns with wearable sensors. *PLoS ONE*, **6**(2), e17144.
- Isella, L., Stehlé, J., Barrat, A., Cattuto, C., Pinton, J.-F., & Van den Broeck, W. (2011b). What's in a crowd? Analysis of face-to-face behavioral networks. *Journal of Theoretical Biology*, **271**(1), 166–180.
- Karsai, M., Kivela, M., Pan, R. K., Kaski, K., Kertesz, J., Barabási, A. L., & Saramäki, J. (2011). Small but slow world: How network topology and burstiness slow down spreading. *Physical Review E*, **83**(2), 025102.
- Kitsak, M., Gallos, L. K., Havlin, S., Liljeros, F., Muchnik, L., Stanley, H. E., & Makse, H. A. (2010). Identification of influential spreaders in complex networks. *Nature Physics*, **6**(11), 888–893.
- Lee, S., Rocha, L. E. C., Liljeros, F., & Holme, P. (2012). Exploiting temporal network structures of human interaction to effectively immunize populations. *PLoS ONE*, **7**(5), e36439.
- Machens, A., Gesualdo, F., Rizzo, C., Tozzi, A., Barrat, A., & Cattuto, C. (2013). An infectious disease model on empirical networks of human contact: Bridging the gap between dynamic network data and contact matrices. *BMC Infectious Diseases*, **13**(1), 185.
- Maslov, S., & Sneppen, K. (2002). Specificity and stability in topology of protein networks. *Science*, **296**(5569), 910–913.
- Merler, S., & Ajelli, M. (2010). The role of population heterogeneity and human mobility in the spread of pandemic influenza. *Proceedings of the Royal Society B-Biological Sciences*, **277**(1681), 557–565.
- Mossong, J., Hens, N., Jit, M., Beutels, P., Auranen, K., Mikolajczyk, R., . . . Edmunds, W. J. (2008). Social contacts and mixing patterns relevant to the spread of infectious diseases. *PLoS Medicine*, **5**(3), e74.
- Onnela, J.-P., Saramäki, J., Hyvönen, J., Szabó, G., de Menezes, M. A., Kaski, K., . . . Kertész, J. (2007). Analysis of a large-scale weighted network of one-to-one human communication. *New Journal of Physics*, **9**(6), 179.
- Opsahl, T., Agneessens, F., & Skvoretz, J. (2010). Node centrality in weighted networks: Generalizing degree and shortest paths. *Social Networks*, **32**(3), 245 – 251.
- Pastor-Satorras, R., & Vespignani, A. (2002). Immunization of complex networks. *Physical Review E*, **65**(Feb), 036104.
- Penn, A., Desyllas, J., & Vaughan, L. (1999). The space of innovation: Interaction and communication in the work environment. *Environment and Planning B: Planning and Design*, **26**(2), 193–218.
- Pfitzner, R., Scholtes, I., Garas, A., Tessone, C. J., & Schweitzer, F. (2013). Betweenness preference: Quantifying correlations in the topological dynamics of temporal networks. *Physical Review Letters*, **110**(May), 198701.
- Read, J. M., Edmunds, W. J., Riley, S., Lessler, J., & Cummings, D. A. T. (2012). Close encounters of the infectious kind: Methods to measure social mixing behaviour. *Epidemiology and Infection*, **140**(12), 2117–2130.
- Sailer, K., & McCulloh, I. (2012). Social networks and spatial configuration—how office layouts drive social interaction. *Social Networks*, **34**(1), 47–58.
- Salathé, M., & Jones, J. H. (2010). Dynamics and control of diseases in networks with community structure. *PLoS Computational Biology*, **6**(4), e1000736.

- Salathé, M., Kazandjieva, M., Lee, J. Woo, L., Philip, F., Marcus W., & Jones, J. H. (2010). A high-resolution human contact network for infectious disease transmission. *Proceedings of the National Academy of Sciences*, **107**(51), 22020–22025.
- Scholtes, I., Wider, N., Pfitzner, R., Garas, A., Tessone, C. J., & Schweitzer, F. (2014). Causality-driven slow-down and speed-up of diffusion in non-Markovian temporal networks. *Nature Communications*, **5**, 5024.
- Smieszek, T., Fiebig, L., & Scholz, R. (2009). Models of epidemics: When contact repetition and clustering should be included. *Theoretical Biology and Medical Modelling*, **6**(1), 11.
- Smieszek, T., & Salathé, M. (2013). A low-cost method to assess the epidemiological importance of individuals in controlling infectious disease outbreaks. *BMC Medicine*, **11**(1), 35.
- Starnini, M., Machens, A., Cattuto, C., Barrat, A., & Pastor-Satorras, R. (2013). Immunization strategies for epidemic processes in time-varying contact networks. *Journal of Theoretical Biology*, **337**(0), 89–100.
- Stehlé, J., Voirin, N., Barrat, A., Cattuto, C., Isella, L., Pinton, J.-F., . . . Vanhems, P. (2011a). High-resolution measurements of face-to-face contact patterns in a primary school. *PLoS ONE*, **6**(8), e23176.
- Stehlé, J., Voirin, N., Barrat, A., Cattuto, C., Colizza, V., Isella, L., . . . & Vanhems, P. (2011b). Simulation of an SEIR infectious disease model on the dynamic contact network of conference attendees. *BMC Medicine*, **9**(1), 87.
- Stopczynski, A., Sekara, V., Sapiezynski, P., Cuttone, A., Madsen, M. M., Larsen, J. E., & Lehmann, S. (2014). Measuring large-scale social networks with high resolution. *PLoS ONE*, **9**(4), e95978.
- Vanhems, P., Barrat, A., Cattuto, C., Pinton, J.-F., Khanafer, N., Régis, C., . . . Voirin, N. (2013). Estimating potential infection transmission routes in hospital wards using wearable proximity sensors. *PLoS ONE*, **8**(9), e73970.
- Vu, L., Nahrstedt, K., Retika, S., & Gupta, I. (2010). Joint Bluetooth/Wifi scanning framework for characterizing and leveraging people movement in University campus. In *MSWIM 2010: Proceedings of the 13th ACM International Conference on Modeling, Analysis, and Simulation of Wireless and Mobile Systems*. 1515 Broadway, New York, NY 10036-9998 USA: ASSOC Computing Machinery, for ACM SIGSIM, pp. 257–265.
- Wasserman, S., & Faust, K. (1994). *Social Network Analysis: Methods and Applications*. Cambridge: Cambridge University Press.
- Zhang, Y., Wang, L., Zhang, Y.-Q., & Li, X. (2012). Towards a temporal network analysis of interactive WiFi users. *Europhysics Letters*, **98**(6), 68002.